Canadian Mineralogist
Vol. 29, pp. 435-452 (1991)

C–O–H–N FLUID EVOLUTION AT SAINT-ROBERT, QUEBEC: IMPLICATIONS FOR W–Bi–Ag MINERAL DEPOSITION

SERGIO CATTALANI AND ANTHONY E. WILLIAMS-JONES
Mineral Exploration Research Institute and Department of Geological Sciences, McGill University,
3450 University Street, Montreal, Quebec H3A 2A7

ABSTRACT

The Saint-Robert deposit consists of quartz ± scheelite ± cosalite ± argentiferous galena ± sphalerite-bearing veins, spatially associated with a felsic dyke swarm in steeply dipping calcareous and carbonaceous sedimentary rocks. A coincident magnetic anomaly and thermal metamorphic zone reflect an unexposed granitic stock. Pervasive and vein-localized argillic-phyllic alteration accompanied mineralization. Early subvertical veins define a central W-rich zone, a northern Bi-bearing zone and a southern Pb–Zn–Ag zone. Late subhorizontal scheelite-bearing veins occur in the central and northern zones. Mineralization was associated with aqueous-carbonic fluids. Primary and pseudosecondary fluid inclusions show a wide range of ratios of aqueous and carbonic phases. The carbonic phases consist of variable proportions of CO_2, CH_4 and N_2. Fluid inclusions from subvertical and subhorizontal scheelite-bearing veins have the highest concentrations of CH_4 and are the only ones to contain N_2. The aqueous phase has a uniformly low salinity. Temperatures based on oxygen isotope fractionation between quartz and scheelite are approximately 240°C for subvertical veins and 200°C for subhorizontal veins. Isochore projections for aqueous and carbonic fluid inclusions predict entrapment pressures of 600–1100 bars. The isotopic composition of oxygen calculated for the ore fluid is consistent with that of meteoric water. The distribution of C–O–H species implies disequilibrium and immiscibility in the source region. A model is proposed in which a meteoric-water-dominated hydrothermal system is initiated by the cooling of a granitic pluton. According to this model, the hydrothermal fluids interacted with calcareous and organic-matter-rich sediments and dissolved metals, sulfur and carbonic volatile species, which they carried to vertically higher levels. Metal deposition is interpreted to have occurred as a result of pH increase through neutralization of the ore fluids by calcareous host-rocks and possibly also effervescence of the carbonic phase.

Keywords: C–O–H–N fluid inclusions, immiscibility, disequilibrium, W–Bi–Ag veins, oxygen isotopes, felsic dykes, phyllic–argillic alteration, Saint-Robert, Québec.

SOMMAIRE

Le gisement de Saint-Robert (Québec) consiste en des filons de quartz ± scheelite ± cosalite ± galène argentifère ± sphalérite, associés à un essaim de dykes felsiques qui recoupent des sédiments calcareux et carbonacés à pendage abrupt. Une anomalie magnétique qui coïncide avec une zone de métamorphisme de contact reflète la présence d'un amas granitique en profondeur. Une altération pénétrante et répandue, à caractère argillique–phyllique, est associée à la minéralisation. Des fissures quasi-verticales et précoces constituent une zone centrale tungstenifère, une zone au nord riche en Bi, et une zone au sud riche en Pb–Zn–Ag. D'autres fissures quasi-horizontales et tardives, riches en W, recoupent les zones du centre et du nord. La minéralisation était associée à des fluides à la fois aqueux et carboniques. Les inclusions fluides d'origines primaire et pseudo-secondaire demontrent un rapport des phases eau – fluide carbonique très variable. Le fluide carbonique montre des proportions variables de CO_2, CH_4 et N_2. Les inclusions fluides provenant de fissures quasi-verticales et quasi-horizontales minéralisées en scheelite contiennent les concentrations de CH_4 les plus importantes, et sont les seules à contenir du N_2. La phase aqueuse a une faible salinité. Le fractionnement isotopique de l'oxygène entre le quartz et la scheelite indique des températures d'environ 240° et 200°C pour les fissures quasi-verticales et quasi-horizontales, respectivement. La projection d'isochores pour les inclusions fluides aqueuses et carboniques indiquent une pression de piégeage de 600 à 1100 bars. La composition isotopique de l'oxygène que nous attribuons au fluide minéralisateur concorde avec celle de l'eau météorique. La distribution des espèces C–O–H implique le déséquilibre et l'immiscibilité de ces phases à la source. Nous proposons un modèle dans lequel un système hydrothermal dominé par l'eau météorique est activé par le refroidissement d'un amas granitique. Ces fluides ont réagi avec des sédiments calcareux et riches en matière organique, et ont ainsi dissous des métaux, du soufre et des espèces carboniques volatiles, qu'ils ont ensuite transportés à des niveaux supérieurs. La mise en place des métaux se serait produite lors d'une augmentation du pH par la neutralisation des fluides minéralisateurs en raison de leur interaction avec des roches calcaires, et peut-être aussi par la libération d'une phase carbonique par effervescence.

Mots-clés: inclusions fluides C–O–H–N, immiscibilité, déséquilibre, minéralisation à W–Bi–Ag, isotopes d'oxygène, dykes felsiques, altération phyllique-argillique, Saint-Robert, Québec.

INTRODUCTION

The occurrence of carbonic-species-bearing fluid inclusions has been documented for a large number of granite-associated, vein-type, scheelite-bearing mineral deposits (*e.g.*, Higgins 1985, Mangas & Arribas 1988, Ramboz *et al.* 1985, Seal *et al.* 1987, Shepherd & Waters 1984, So *et al.* 1983a, b). Carbon dioxide is the principal carbonic species, but methane has been reported for several deposits (*e.g.*, Ramboz *et al.* 1985, So *et al.* 1983b). In a small number of cases, nitrogen also is present in the carbonic phases (*e.g.*, Ramboz *et al.* 1985). Although the association of C–O–H ± N fluid species with the above class of deposits is now well established, the role of these fluids in the mineralizing process is still poorly understood.

In this paper we report the results of a fluid inclusion study of a small, granite-associated, vein-type scheelite deposit in which primary and pseudosecondary fluid inclusions contain high and variable proportions of carbonic species, and in which the occurrence of scheelite correlates strongly with the presence of nitrogen in the carbonic phase(s). These observations are used to develop a model in which meteoric fluids, in circulation around a cooling granite pluton, leached tungsten from organic-matter-rich sediments and deposited

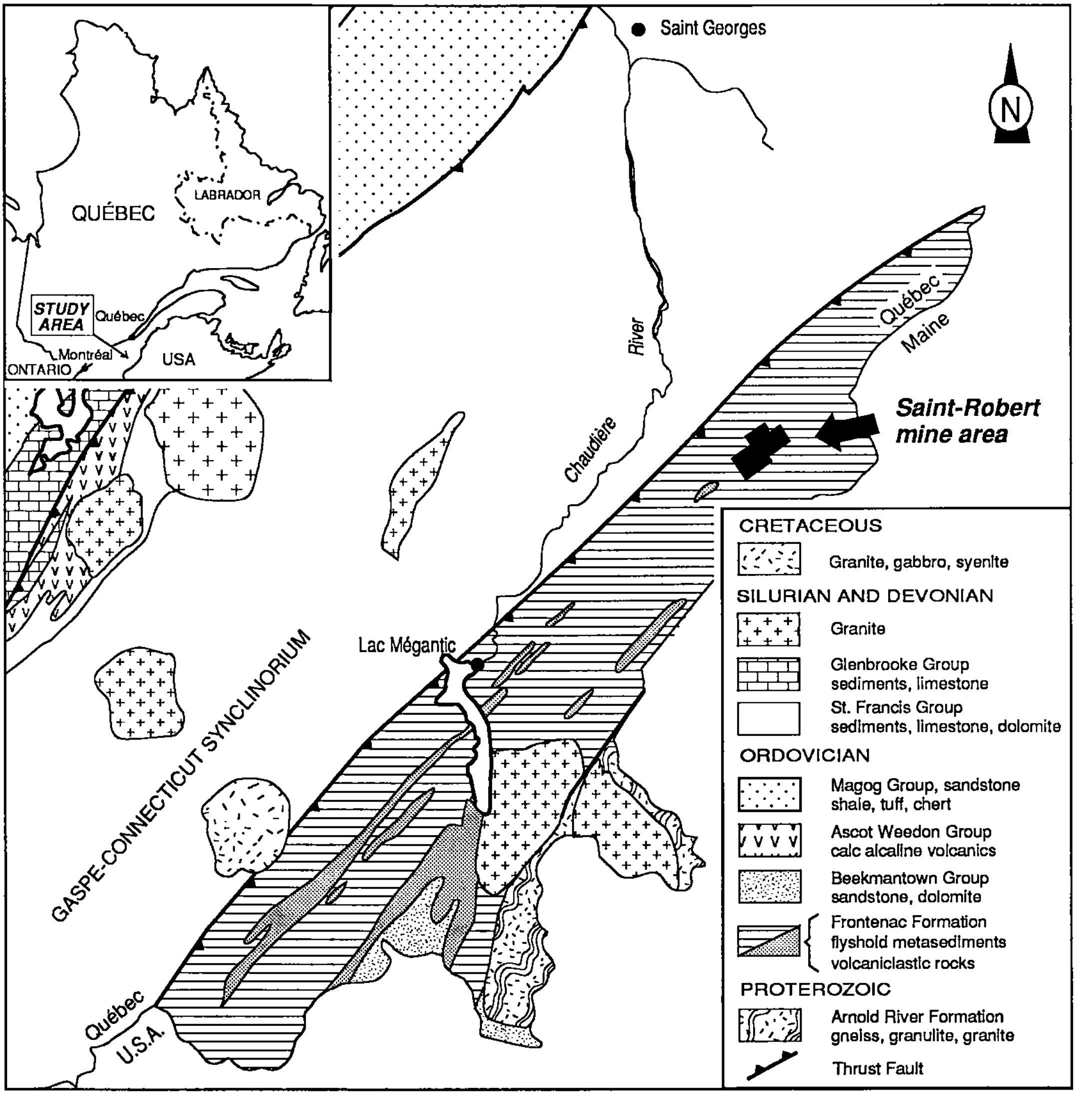

FIG. 1. Map showing the location and regional geological setting of the Saint-Robert deposit. Modified after Gauthier (1985).

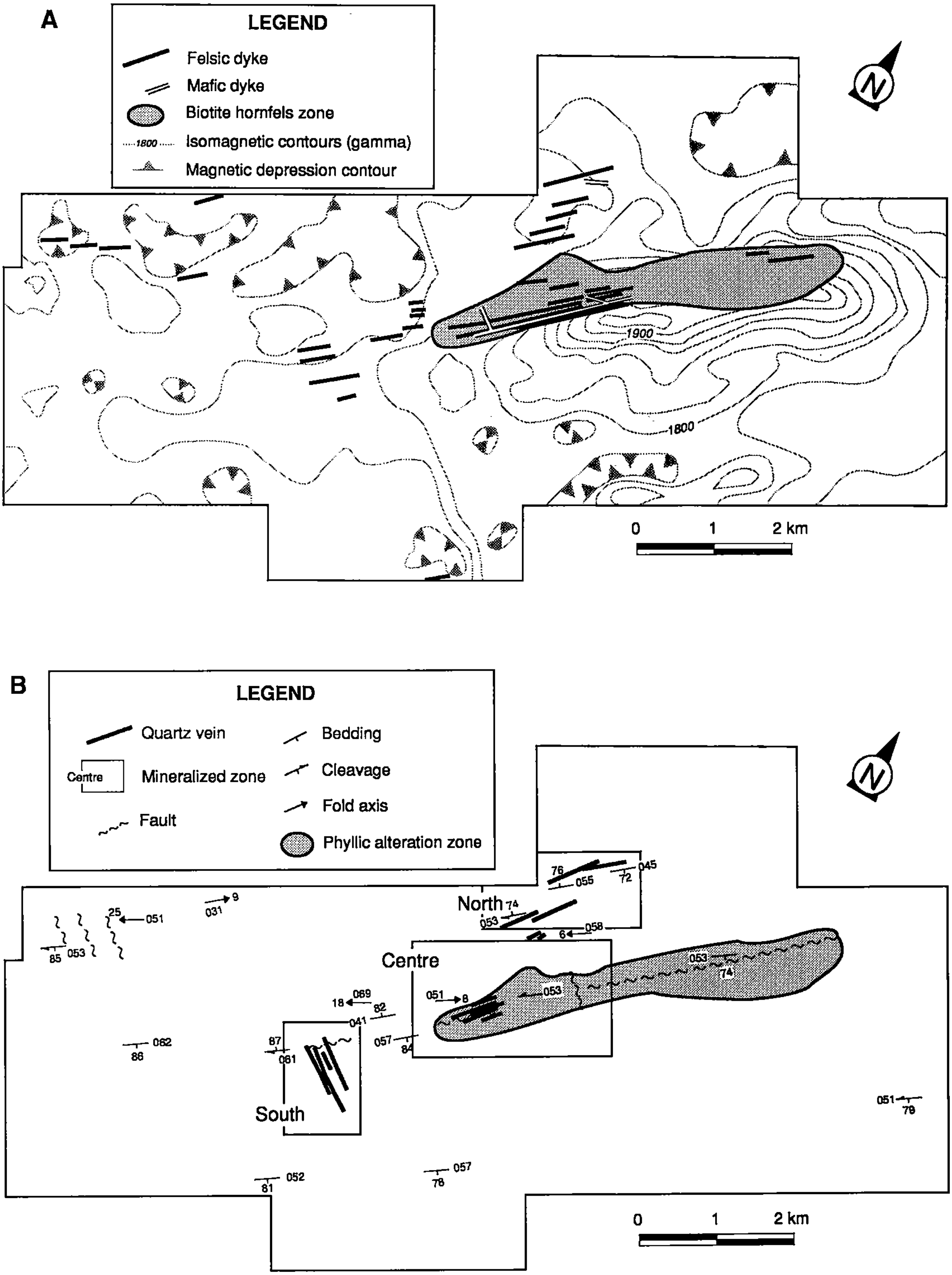

FIG. 2. Maps showing A) magnetic anomalies, distribution of dykes and the location of the thermal metamorphic zone, and B) distribution of veins, pervasive alteration and faults.

scheelite in response to a pH increase caused by wallrock neutralization of the ore fluids and possibly also effervescence of the carbonic phase.

GEOLOGICAL SETTING

The Saint-Robert deposit, located about 35 km northeast of Lac Mégantic, Québec, occurs along the northwestern flank of the Appalachian structural province, immediately to the south of the fault-bounded contact between the Boundary Mountain anticlinorium and the Gaspé – Connecticut Valley synclinorium (Fig. 1). Scheelite-bearing veins were originally discovered at Saint-Robert during the late 19th century and are of historical importance as the first reported occurrence of scheelite in Canada (*cf.* Little 1959). However, there was no serious exploration of the area until the 1950s, when numerous scheelite-bearing quartz veins were delineated at the surface and precious-metal mineralization at depth. The deposit was brought into production briefly in 1958.

The mineralized quartz veins are hosted by rocks of the Early Ordovician Frontenac Formation. The latter comprise turbiditic sedimentary rocks that consist largely of alternating light to medium grey quartzites, medium to dark grey slates, and light to medium brownish calcareous metagreywackes. Thin, contorted interbeds of black graphitic slate are locally present in the section.

The deposit is spatially associated with a swarm of ENE-striking felsic dykes of granodioritic to granitic composition that were emplaced during an episode of Acadian calc-alkaline intrusive activity (Bourne 1989, Harron 1976). The dykes are concentrated in the central part of the mine area and coincide with a broad positive magnetic anomaly that may represent a larger intrusive body at depth (Fig. 2A). Rare lamprophyre dykes of possible Cretaceous age cross-cut the felsic dykes and quartz veins.

Sedimentary strata were isoclinally folded during the Middle Devonian Acadian orogeny and display a conspicuous, steeply dipping, bedding-plane cleavage. A system of vertical faults parallels the principal foliation (northeast) and cuts through the center of the deposit (Fig. 2B). This fault system has a strike length of at least 2.5 km and is coincident with a set of thick felsic dykes (up to 20 m thick). Displacement along the faults appears to have been dominantly dip-slip in character, with downthrow to the north. A small number of apparently subvertical, late, minor faults occur nearly normal to the main fault-system in the western and central parts of the mine area.

Regional metamorphism was restricted to the lower greenschist facies. A thermal metamorphic overprint resulted in a roughly oval-shaped zone of brownish biotite hornfels that coincides spatially with the area of major concentration of dykes and the magnetic anomaly (Fig. 2A).

Moderate to intense pervasive hydrothermal alteration postdated thermal metamorphism, and was developed in a zone that is roughly coincident with the thermal metamorphic zone. The overall pattern of alteration is clearly fault-controlled and may be described as consisting of a narrow proximal argillic facies in, and adjacent to, the main fault system, within a broader phyllic halo (Fig. 2B).

The spatial coincidence of mineralized veins, felsic dyke swarm, magnetic anomaly, thermal metamorphic zone and hydrothermal alteration halo suggests that scheelite deposition was penecontemporaneous with and genetically related to the emplacement of an unexposed granitic pluton.

MINERALIZATION AND PARAGENESIS

The mineralization at Saint-Robert is hosted by veins of massive quartz containing small quantities of calcite and sericite as late, fracture-filling phases. The veins range in thickness from 10 cm to almost 1 m, and may reach 150 m in length. A characteristic greenish halo representing weak to intense phyllic alteration surrounds most veins and consists of a fine-grained assemblage of quartz, sericite, illite, calcite, pyrite and rutile. Cross-cutting relationships indicate that vein formation postdated felsic dyke emplacement. The veins commonly show branching, pinching and swelling, variations in strike, signs of fracturing and resealing, and the development of vugs.

Mineralized veins are of two main types, subvertical and subhorizontal, and occur in three distinct zones located in the north, south and central parts of the mine area (Fig. 2B). Subvertical veins occur in all three zones and make up the bulk of the veining. Subvertical veins in the North and Centre zones are parallel to the foliation, whereas those in the South zone strike almost perpendicular to foliation and dip steeply to the northeast. It is unclear whether subvertical veins in the South zone are temporally equivalent to those in the North and Centre zones. Subhorizontal veins are restricted to the Centre and North zones and, on the basis of cross-cutting relationships, are younger than the subvertical veins.

The ore mineral assemblage comprises scheelite, cosalite ($Pb_2Bi_2S_5$), argentiferous galena, sphalerite, pyrite, and minor chalcopyrite and pyrrhotite. Scheelite is concentrated mainly in the Centre zone veins and is represented by two distinct episodes of mineralization. Early scheelite occurs in subvertical

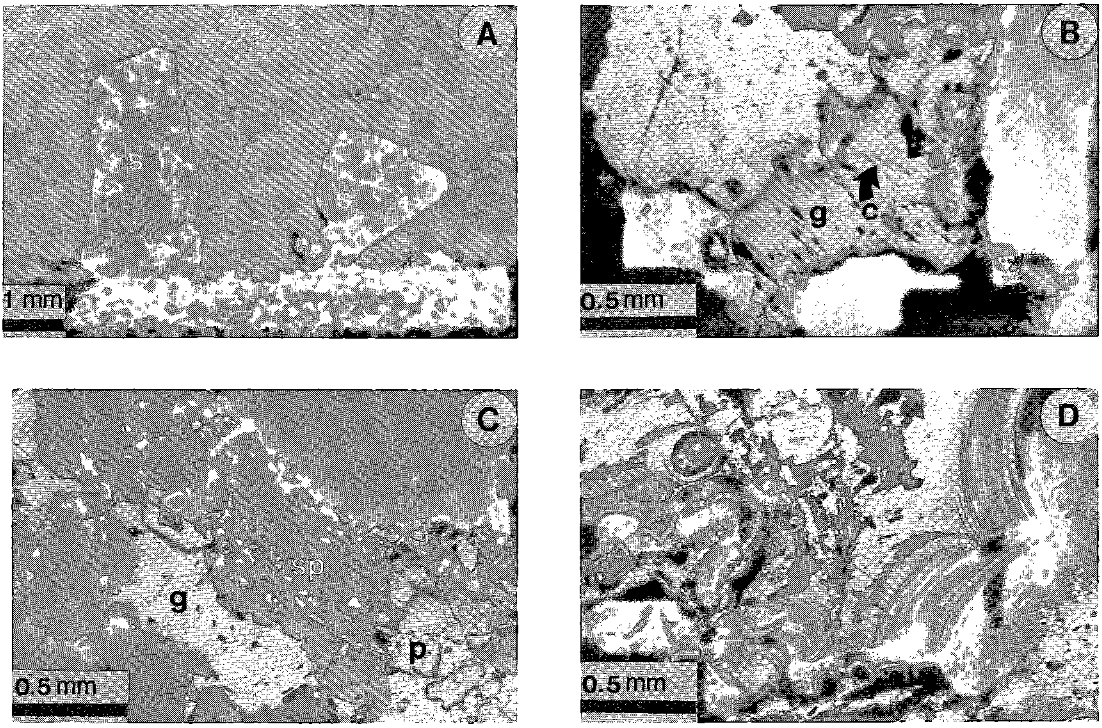

FIG. 3. Photomicrographs showing A) early euhedral scheelite (s) crystals at the margin of a quartz vein in the Centre zone; B) a needle of cosalite (c) in a crystal of galena (g); C) a sulfide-rich calcite veinlet containing sphalerite (sp), interstitial galena (g) and minor pyrite (p) cross-cutting a subvertical quartz vein from the Centre zone; D) colloform pyrite in a vug in a subvertical vein from the South zone.

veins as euhedral crystals measuring several mm across, adjacent to vein–wallrock contacts (Fig. 3A). Grains of late scheelite are anhedral to euhedral, and are found in subhorizontal veins and the cores of some subvertical veins, where they are commonly associated with late, fracture-filling calcite. Subhorizontal veins in the Centre zone contain the highest concentrations (up to 30% by volume) of scheelite, which is dominantly late.

Cosalite is the main economic sulfide mineral in subvertical North zone veins, occurs in only minor quantities in Centre zone veins, and is absent from South zone veins. Cosalite forms long (up to 10 cm), acicular crystals that are commonly arranged as fans and bundles that radiate inward from the vein–wallrock contact. In Centre zone veins, cosalite occurs exclusively as acicular inclusions within crystals of galena (Fig. 3B).

Galena and sphalerite commonly occur together within calcite-filled microveinlets that cut quartz in subvertical veins (Fig. 3C) and as euhedral crystals that line the walls of vugs and cavities in subvertical South zone veins. The concentration of these minerals is highest in the South zone veins. The galena is argentiferous and represented an important source of silver during the period of mine production; no other Ag-bearing minerals have been identified. Sphalerite is usually dark brown.

It is possible to distinguish at least three distinct generations of pyrite: an early stage found within secondary fractures in subvertical veins, a later stage occurring within calcite-filled microveinlets (Fig. 3C) that cross-cut the main stage of quartz and secondary fractures within them, and a stage that lines vugs in South zone veins. Pyrite occurs as cubes in all three stages, and also as a colloform mineral in the vug stage (Fig. 3D). Replacement textures show that, in all cases, pyrite predated sphalerite and galena. Chalcopyrite and pyrrhotite occur in minor amounts as secondary anhedral blebs within sphalerite and pyrite.

Subvertical veins within the deposit form a southern, Ag–Pb–Zn-rich zone, a central, W-rich zone and a northern, Bi–Pb-rich zone. Later subhorizontal veins served to enrich the Centre and North zones in tungsten. A generalized paragenetic

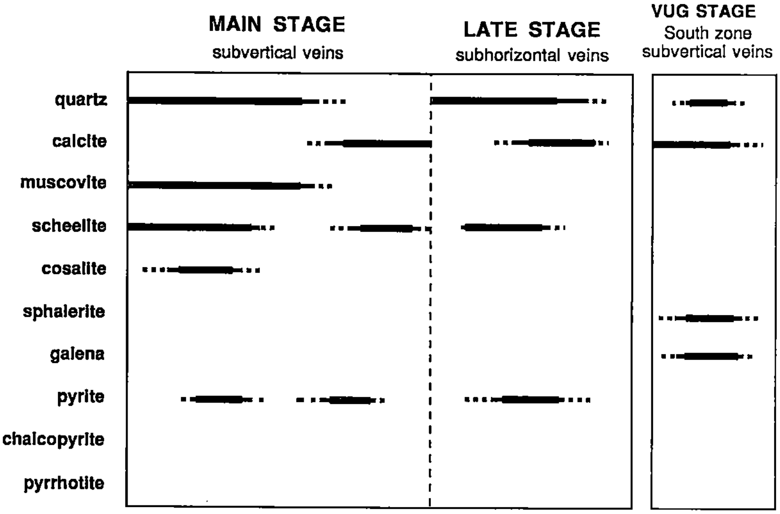

FIG. 4. Mineral paragenesis in the veins.

sequence for the various episodes of mineralization observed at Saint-Robert is presented in Figure 4.

ANALYTICAL TECHNIQUES

Microthermometric analysis of fluid inclusions was performed using an S.G.E. Model III heating-freezing stage based on a USGS design (Hollister *et al.* 1981, Werre *et al.* 1979). Temperatures of the various phase-changes were measured using a chrome-alumel thermocouple, and were recorded on a digital indicator. The thermocouple was calibrated for temperatures between -100° and 500°C using the melting points of a variety of organic and inorganic compounds and metals. Reported temperatures are accurate to ±0.1°C in the subzero range and ±3°C at the highest temperatures. The heating rate was maintained below 1°C per minute to minimize the chance of metastable phase-changes.

A number of fluid inclusions were analyzed at McGill University using a Yvon-Jobin Raman spectrometer, equipped with a Ramanor U-1000 monochrometer and a Spectra Physics 164 ionized 6-watt argon laser. The exciting frequency used in this study was 514.5 μm at a laser-beam power of 300 to 500 mW. The host mineral in all cases was quartz. All inclusions were analyzed for the following species: CO_2, CH_4, N_2, NH_3, NO, H_2S, and SO_2. Only CO_2, CH_4, and N_2 were detected. The relative proportions of these species were determined using the following equation:

$$Ca/Cb = Aa/Ab * Fa/Fb$$

where C refers to concentration, A to peak area, F to a pressure-dependent gas-scattering efficiency factor, and a and b to the gas species analyzed (Pasteris *et al.* 1988). The F-factors were taken from Wopenka & Pasteris (1987). The validity of these instrument-specific F-factors for data collected at McGill was checked by analyzing CO_2-N_2-O_2 gas standards supplied by J.D. Pasteris. Our calculated compositions for these standards are within 3 mole % of the compositions determined by Pasteris on the Washington University instrument.

Isotopic analyses of sulfur and oxygen were performed at McMaster University by Drs. C. C. McMullen and H. P. Schwarcz, respectively. Analyses were carried out on a non-commercial, 6″, 90° magnetic sector mass spectrometer, equipped with a double-ion collector system. The analytical precision is estimated to be 0.4¡ for sulfur and 0.1¡ for oxygen. The standard stable isotope notation is used here. Reference standards are the Cañon Diablo troilite for sulfur (Thode *et al.* 1961) and SMOW (Standard Mean Ocean Water) for oxygen (Craig 1957, 1961).

THE FLUID INCLUSIONS

Petrography

Fluid inclusions were investigated from samples representing the various veins in the Saint-Robert deposit. The majority of fluid inclusions suitable for microthermometry were found in quartz. A small number of inclusions in scheelite and sphalerite also were analyzed.

The majority of inclusions are aqueous-carbonic. Small proportions of carbonic and aqueous inclusions were observed in samples from all vein sets.

Aqueous-carbonic inclusions contain two or three phases (aqueous liquid ± carbonic liquid ± carbonic vapor) and vary from a few μm to almost 100 μm in diameter. A high proportion of aqueous-carbonic inclusions are primary or pseudosecondary in origin; they occur in isolation or along growth zones. Many display an equant to slightly elongate negative-crystal morphology. Only a small proportion of aqueous-carbonic inclusions are clearly secondary. Aqueous-carbonic inclusions, even within the same growth-zone, display a highly variable ratio of volume of carbonic fluid to volume of aqueous fluid at room temperature. Carbonic inclusions are mainly one phase at room temperature and occur in close spatial association with aqueous-carbonic inclusions. Aqueous inclusions are two-phase, with liquid-to-vapor ratios greater than 9:1, and range from a few μm to well over 100 μm in diameter. They are commonly irregular in shape, occur along healed fractures, and are mainly secondary in origin. A small proportion of aqueous inclusions occur in clusters with carbonic and aqueous-carbonic inclusions and may be primary.

Microthermometric data: aqueous-carbonic and carbonic inclusions

Carbonic inclusions and the carbonic phase of aqueous-carbonic inclusions display similar microthermometric behavior and have accordingly been treated together. The final melting temperature of carbonic ice ($TmCO_2$) falls well below that of pure CO_2 for the majority of aqueous-carbonic and carbonic inclusions. $TmCO_2$ for inclusions from veins in the South and Centre zones ranges from about -64° to -56.6°C; for inclusions from veins in the North zone, it ranges from about -60° to -56.6°C; and for inclusions from subhorizontal veins, it shows a bimodal distribution, with peaks at -67° to -63°C and -60° to -56.6°C (Fig. 5). The low melting temperatures of carbonic ice in many of the inclusions suggest a complex carbonic fluid consisting of CO_2 and CH_4 or N_2 (or both).

A clathrate was observed to form in most aqueous-carbonic inclusions. This phase decomposed (TmC) at temperatures between +5° and +15° C, the highest temperatures being for two inclusions from subhorizontal veins (Fig. 5). Inclusions from subvertical veins in each of the zones show rough correlations of increasing TmC with decreasing $TmCO_2$ (Fig. 5). This correlation is most obvious for inclusions from South zone veins. There is no apparent correlation between TmC and $TmCO_2$ in inclusions from subhorizontal veins.

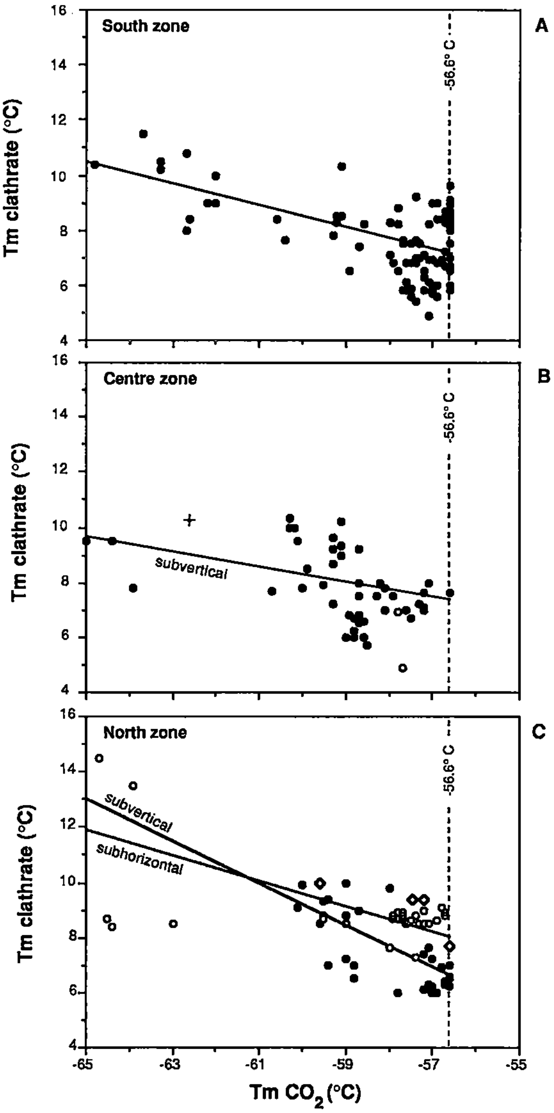

FIG. 5. The melting temperature of carbonic ice ($TmCO_2$) *versus* the melting temperature of clathrate (TmC) for aqueous-carbonic inclusions. Closed circles, crosses and diamonds represent inclusions hosted by quartz, sphalerite and scheelite, respectively, in subvertical veins; open circles represent quartz-hosted inclusions in subhorizontal veins. Solid lines represent least-square regressions of the data.

The carbonic phases in aqueous-carbonic and carbonic inclusions in subvertical veins from the South and Centre zones homogenize, with rare exception, to liquid [$ThCO_2$ L–V (L)], and at temperatures ranging from about -25° to +25°C; in North zone veins, they homogenize to liquid over a slightly more restricted range in temperature, from about -15° to +20°C. However, aqueous-carbonic and carbonic inclusions in subhorizontal veins display a bimodal distribution of $ThCO_2$ L–V (L) of the carbonic phases, from -55° to -15°C and from -5° to +20°C.

The aqueous phase in aqueous-carbonic inclusions begins to melt in the range -35° to -16°C and is finally molten between -7° and -1°C, which suggests a low-salinity fluid containing NaCl, dissolved carbonic species, and possibly other salts. Salinities of aqueous-carbonic inclusions were calculated from the clathrate melting temperature (TmC) using the equation of Bozzo *et al.* (1973). Average salinities for inclusions from the various sets of veins were determined using the TmC value at the -56.6°C $TmCO_2$ intercept on a regression of TmC *versus* $TmCO_2$ (Fig. 5). These salinities are 5.6, 5.4, and 7.1 wt.% NaCl eq. for subvertical veins in the South, Centre and North zones, respectively, and 4.3 wt.% NaCl eq. for subhorizontal veins. In a few inclusions, $TmCO_2$ was found to be -56.6°C. The corresponding salinities calculated for these inclusions range from 2.0 to 7.8 wt.% NaCl eq. Nitrogen, which, as will be shown later, is present in some inclusions, has an effect similar to that of NaCl. However, since 1) these inclusions are restricted to Centre zone veins and 2) aqueous-carbonic inclusions in all sets of veins have quite similar calculated salinities, it is reasonable to conclude that the latter are reliable estimates of the concentrations of dissolved salts.

$ThCO_2$ L–V values correlate well with $TmCO_2$ (Fig. 6), which confirms that the carbonic phases contain varying amounts of additional species. These data were used to determine the bulk composition of the carbonic phases following the method of Burruss (1981). The assumption was made that the only additional species is CH_4 or N_2 (this is supported by Raman spectroscopic data presented below), and that because of the similarity in their LV equilibrium curves, the sum of these species can be treated as CH_4-equivalent. The mole fraction of CH_4 + N_2 [$Z_{CH4\ eq.}$] in carbonic inclusions and in the carbonic phase in aqueous-carbonic inclusions so calculated ranges from 0 to 1. Inclusions from subvertical veins in the South and North zones have $Z_{CH4\ eq.}$ less than 0.4 (Fig. 7). Carbonic inclusions in all subhorizontal veins and in subvertical veins from the Centre zone have the highest values of $Z_{CH4\ eq.}$. In subvertical veins from the Centre zone, carbonic inclusions show a bimodal distribution of $Z_{CH4\ eq.}$ values (Fig. 7B).

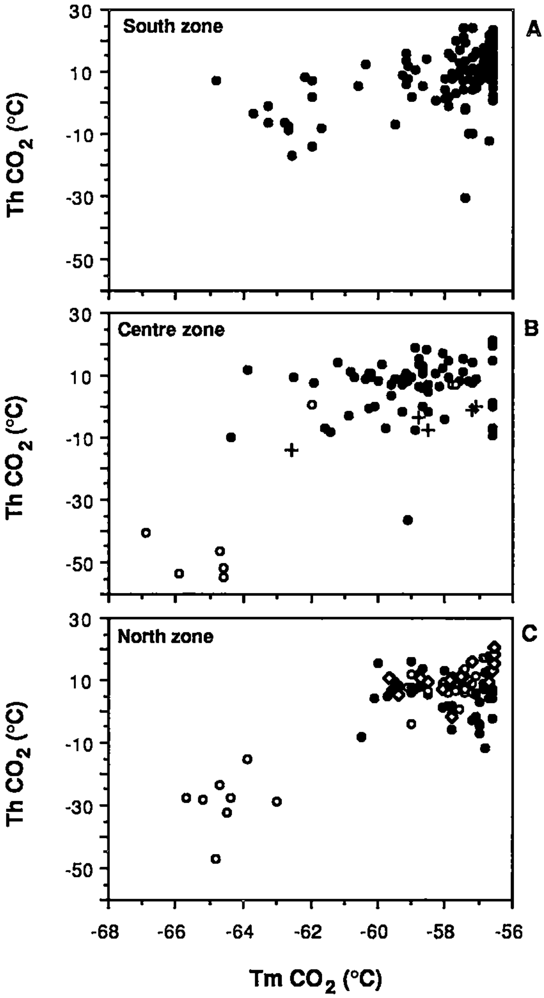

FIG. 6. The melting temperature of carbonic ice ($TmCO_2$) *versus* carbonic phase homogenization temperature ($ThCO_2$ L–V) for carbonic and aqueous-carbonic inclusions. Closed circles, crosses and diamonds represent inclusions hosted by quartz, sphalerite and scheelite, respectively, in subvertical veins; open circles represent quartz-hosted inclusions in subhorizontal veins.

The mole fraction of H_2O, $X(H_2O)$, in aqueous-carbonic inclusions was calculated using visual estimates of the relative volumes of aqueous and carbonic phases at the temperature of homogenization of the carbonic phases (only inclusions with $ThCO_2$ L–V > TmC were considered; the presence of a clathrate leads to erroneous estimates of the density of the carbonic phase), the estimates of $Z_{CH4\ eq.}$, the molar densities of the carbonic phase

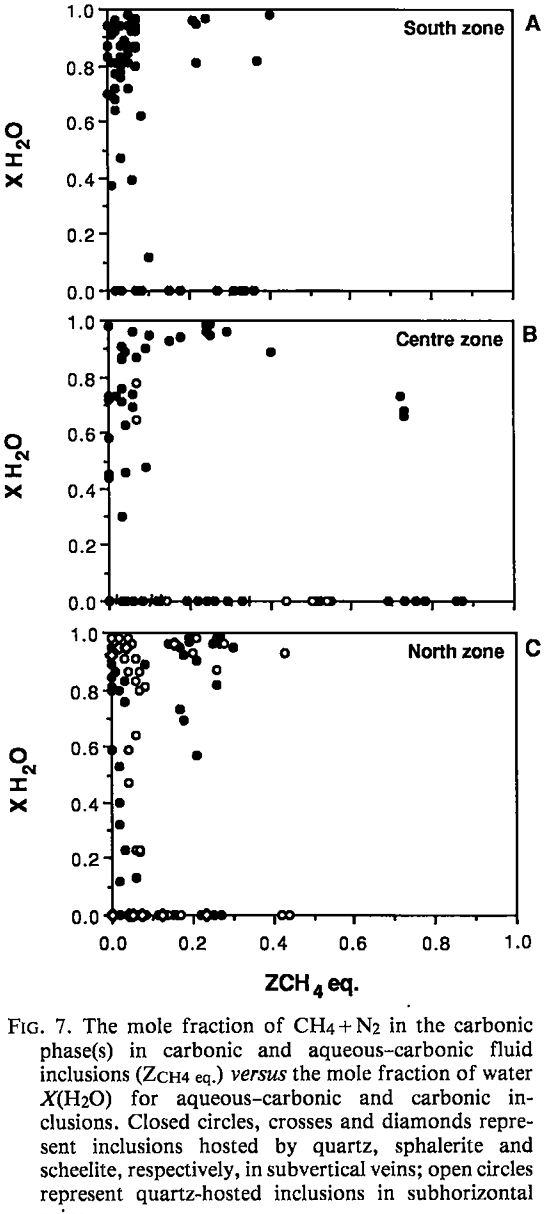

FIG. 7. The mole fraction of CH_4+N_2 in the carbonic phase(s) in carbonic and aqueous-carbonic fluid inclusions ($Z_{CH4\ eq.}$) *versus* the mole fraction of water $X(H_2O)$ for aqueous-carbonic and carbonic inclusions. Closed circles, crosses and diamonds represent inclusions hosted by quartz, sphalerite and scheelite, respectively, in subvertical veins; open circles represent quartz-hosted inclusions in subhorizontal veins.

(Arai *et al.* 1971, Burruss 1981, Parry 1986) and the molar densities of the aqueous phase (Potter & Brown 1977). South zone veins are dominated by inclusions that have a high $X(H_2O)$ (Fig. 7A). In contrast, inclusions from veins in the Centre and North zones show a wide range of $X(H_2O)$, although those with high $X(H_2O)$ are also the most common. In all veins, inclusions with high $Z_{CH4\ eq.}$ have a high $X(H_2O)$.

A large proportion of aqueous-carbonic inclusions decrepitated prior to complete homogenization. Decrepitation temperatures (T_D) are, nonetheless, useful as they represent minimum estimates of the homogenization temperatures, and, as will be shown later, provide even better estimates of the entrapment temperatures. Inclusions in subvertical veins from the North, Centre and South zones homogenize or decrepitate at temperatures in the range 120° to 320°C, and mainly between about 180° and 250°C (Fig. 8). Aqueous-carbonic inclusions in subhorizontal veins homogenize or decrepitate at temperatures ranging from 160° to 300°C, with a possible bimodal distribution in which the main peak occurs between 190° and 210°C, and the secondary peak is from 250° to 270°C.

Microthermometric data: aqueous inclusions

Aqueous inclusions associated with primary and pseudosecondary aqueous-carbonic and carbonic inclusions and those that occur in separate secondary planes show the same range of ice melting temperatures. The initial melting temperatures (Te) range from -35° to -16.5°C and show a well-defined peak between -30° and -22.5°C (Fig. 9A). These temperatures fall well below the stable eutectic temperature for a pure H_2O-NaCl solution (-20.8°C), which suggests the presence of additional species in the aqueous liquid. The most important of these, given the nature of the host rocks (calcareous sediments), probably is $CaCl_2$; the eutectic temperature for the system H_2O-NaCl-$CaCl_2$ is -52.0°C (Crawford 1981).

Final temperatures of ice melting (Tm ice) range from -6.8° to -0.3°C, with a mean of -3.7°C (Fig. 9B), which corresponds to salinities ranging from 0.5 to 10.2 wt.% NaCl eq., with a mean salinity of 5.8 wt.% NaCl eq. (Potter *et al.* 1978). Salinities plotted against homogenization temperatures define a single population; there is no obvious correlation of salinity with temperature (Fig. 10).

Aqueous inclusions associated with aqueous-carbonic and carbonic inclusions homogenize to liquid [Th L-V (L)] at temperatures ranging from 179° to 235°C; aqueous inclusions of clearly secondary origin homogenize to liquid at temperatures between 86° and 197°C (Fig. 11).

RAMAN SPECTROSCOPY

A total of 77 aqueous-carbonic and carbonic fluid inclusions were analyzed by Raman laser spectroscopy. The most common component in the carbonic phases in inclusions from all samples is CO_2, followed in decreasing order by CH_4 and N_2

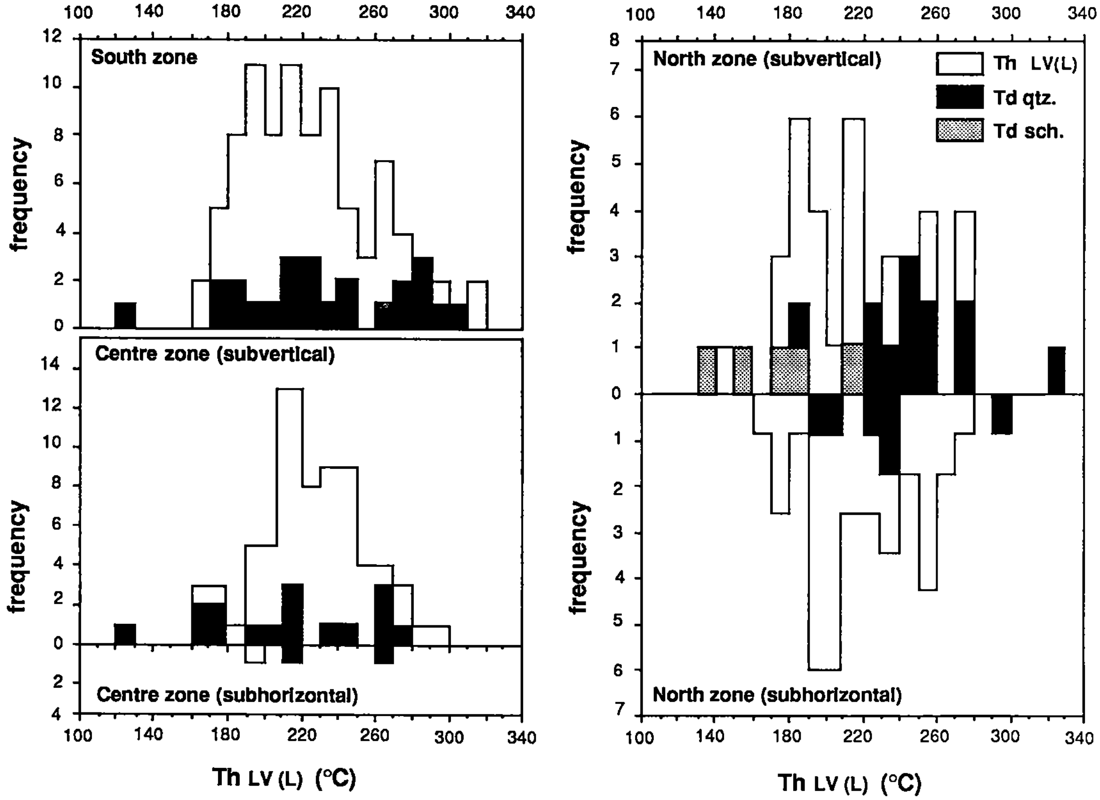

FIG. 8. Histograms of homogenization (white areas) and decrepitation temperatures (black and grey areas) for aqueous–carbonic inclusions.

(Fig. 12). The only inclusions that contain N_2 are in subhorizontal veins and in subvertical veins of the Centre zone. Nitrogen-bearing inclusions in subhorizontal veins all have essentially the same CO_2/CH_4 ratio of approximately 1.5:1, whereas N_2-bearing inclusions in subvertical veins of the Centre zone appear to define a linear trend of increasing N_2 with decreasing $X(CH_4)$. Fluid inclusions from veins in the North and South zones are dominantly CO_2-rich.

OXYGEN ISOTOPES

A total of 22 samples of quartz and four samples of coexisting scheelite were analyzed for their oxygen isotopic compositions. The $\delta^{18}O$ values for quartz and scheelite show similar ranges in all sets of veins. For quartz, the range is from +8.06 to + 12.41‰ ($\bar{x}$ = +9.57‰); for scheelite, $\delta^{18}O$ ranges from -0.6 tp +0.96‰ ($\bar{x}$ +0.15‰) (Table 1).

DISCUSSION

P-T conditions

Temperatures of vein formation were estimated using the oxygen isotopic data and fractionation factors for quartz–water from Clayton *et al.* (1972) and scheelite–water from Wesolowski & Ohmoto (1986). The two samples from subvertical veins in the Centre zone yielded temperatures of 235° and 242°C, and the samples from the subhorizontal veins in the North and Centre zones gave temperatures of 195° and 208°C, respectively (Table 1). These temperatures are within the range of homogenization and decrepitation temperatures for aqueous–carbonic inclusions, which suggests that entrapment occurred at temperatures corresponding to, or below, those of the two-phase boundary.

Experimental data show that at the above temperatures and all geologically reasonable pres-

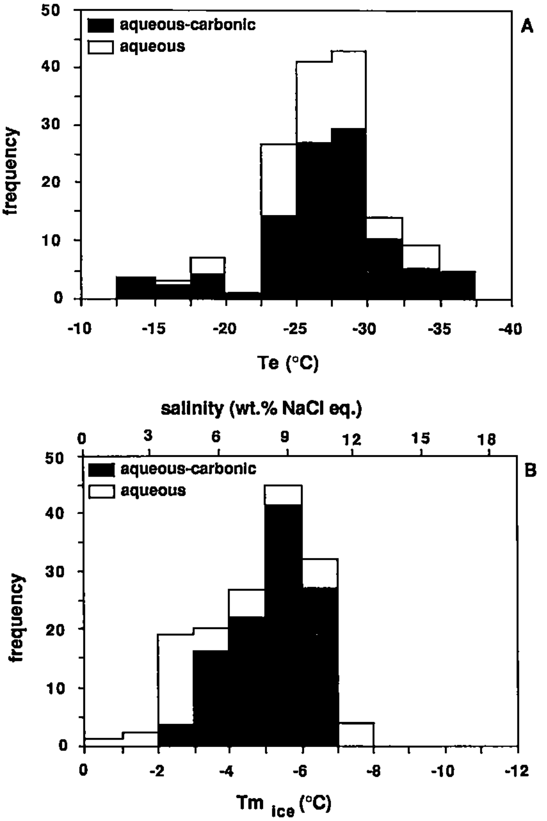

FIG. 9. Histograms of A) eutectic temperatures (Te) and B) final melting temperatures of ice (Tm ice) and calculated salinities of aqueous inclusions (white areas) and the aqueous phase in aqueous-carbonic inclusions (black areas).

sures, there is a wide interval of fluid immiscibility in the CH_4-N_2-absent analogue of the system represented by the Saint-Robert fluids (H_2O-CO_2-$NaCl_{2-8 wt.\%}$; *cf.* Gehrig 1981, Takenouchi & Kennedy 1964, 1965). By analogy with the systems H_2O-CO_2 and H_2O-CO_2-CH_4, the addition of CH_4 to the system H_2O-CO_2-$NaCl_{2-8\ wt.\%}$ would further increase the region of immiscibility (Holloway 1984). A similar effect can be expected from the addition of N_2. Evidence of such immiscibility is provided by the wide range of $X(CO_2)'$ $[X(CO_2)+X(CH_4)+X(N_2)]$ values of aqueous-carbonic inclusions in all sets of veins (Fig. 13). The latter suggests extensive heterogeneous entrapment of variable proportions of separate aqueous and carbonic phases. The high proportion of fluid inclusions decrepitating before homogenization reflects the high internal pressures required to homogenize aqueous-carbonic fluids. The fact that the few inclusions that do homogenize do not appear to define a specific solvus is due, in part,

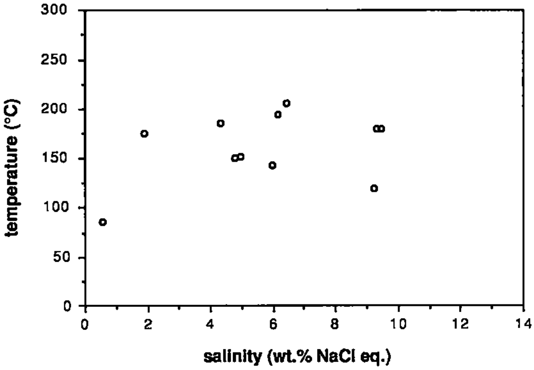

FIG. 10. Homogenization temperature (Th L-V) *versus* salinity (wt.% NaCl eq.) for aqueous inclusions.

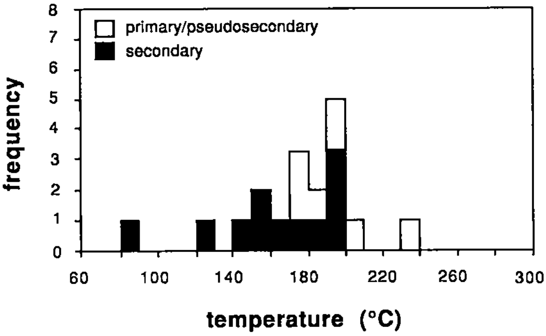

FIG. 11. A histogram of homogenization temperatures (Th L-V) for aqueous inclusions.

TABLE 1. $\delta^{18}O$ COMPOSITIONS AND CALCULATED TEMPERATURES

Sample			$\delta^{18}O$ (‰)	T (°C)
	Qtz	Sch	H_2O	
South Zone				
SC-37b	10.66		+1.22	
SC-50	9.44		0.00	
SC-51	10.69		+1.25	
SC-52	8.73		-0.71	
SC-54	10.70		+1.26	
J82-11-4	9.84		+0.40	
J84-3-2	8.74		-0.70	
Centre Zone				
J83-13-1	10.35		+0.91	
J83-08-9	9.44		0.00	
SC-53	9.46		+0.02	
Lac-NE	10.17	-0.30	+0.73	235
Lac-exit	8.57		-0.87	
Lac-NW	9.27		-0.17	
Lac-SW	9.00		-0.44	
J82-2-2	11.58		+2.14	
J82-1-9	10.58	0.54	+1.14	242
North Zone				
SC-84-49	8.06		-1.38	
SC-84-44	12.32		+2.88	
Subhorizontal				
Lac-SW Flat	12.41	0.96	+2.97	208
SC-84-23	9.14		-2.57	
N.Z. Horiz.	11.31	-0.60	-0.40	195

The isotopic compositions of H_2O were calculated using the quartz-water fractionation line of Clayton et al. (1972), and pertain to temperatures of 240 ° and 200 °C for subvertical and subhorizontal veins, respectively. Temperatures were calculated using the quartz-scheelite geothermometer of Wesolowski & Ohmoto (1986).

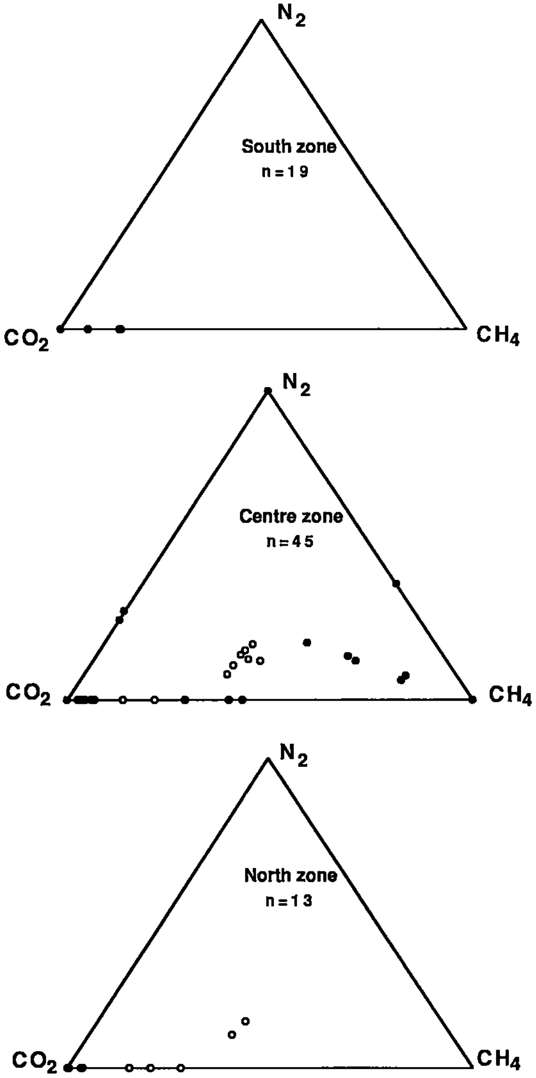

FIG. 12. The composition of the carbonic phase in aqueous-carbonic and carbonic inclusions as determined by Raman spectroscopy. Closed circles represent subvertical veins, and open circles represent subhorizontal veins. The number (n) of inclusions analyzed in each zone is indicated on the corresponding diagram.

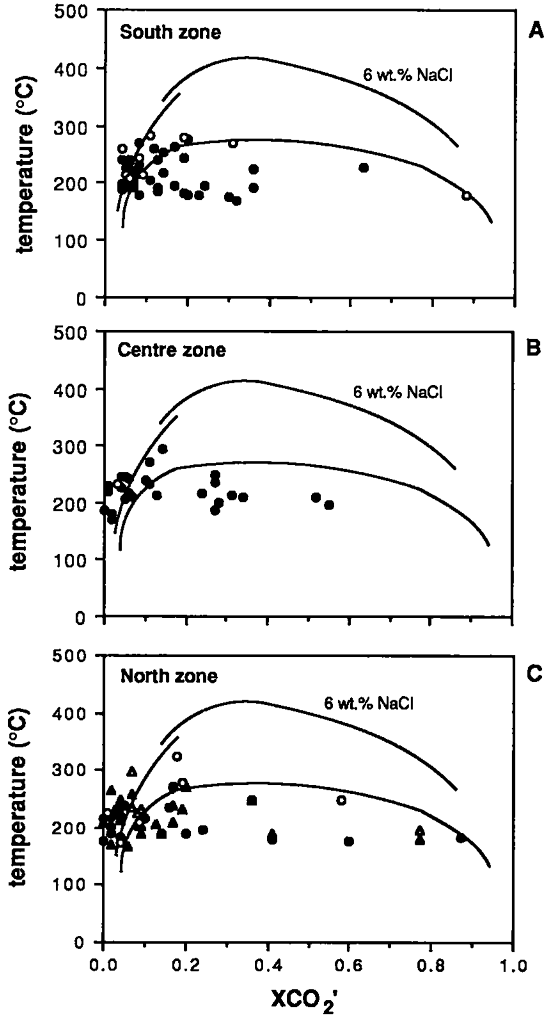

FIG. 13. Homogenization-decrepitation temperature *versus* the mole fraction of carbonic species $X(CO_2)'$ for aqueous-carbonic inclusions. Also shown on the diagram are the 1 kbar solvi for the system H_2O-CO_2-$NaCl_{6\ wt.\%}$ (Takenouchi & Kennedy 1965, Gehrig 1980) and H_2O-CO_2 (Takenouchi & Kennedy 1964). Circles and triangles represent subvertical and subhorizontal veins, respectively. Open and closed symbols represent homogenization and decrepitation, respectively.

to variable salinity, and, in part, to the difficulty in determining Th L-V (V) of inclusions that homogenize by expansion of the carbonic phase [$X(CO_2)' > 0.3$]. Further evidence of fluid immiscibility is provided by the observation that aqueous-carbonic fluid inclusions in the same growth zone also have a wide range of ratios of aqueous to carbonic phases. In a few cases, aqueous inclusions were seen to coexist with carbonic inclusions.

In view of the above, we have estimated the pressure in the Saint-Robert veins by constructing isochores for primary and pseudosecondary aqueous and carbonic fluid inclusions with $X(H_2O)$ values equal to one and zero, respectively. Bounding isochores for the two types of inclusions are

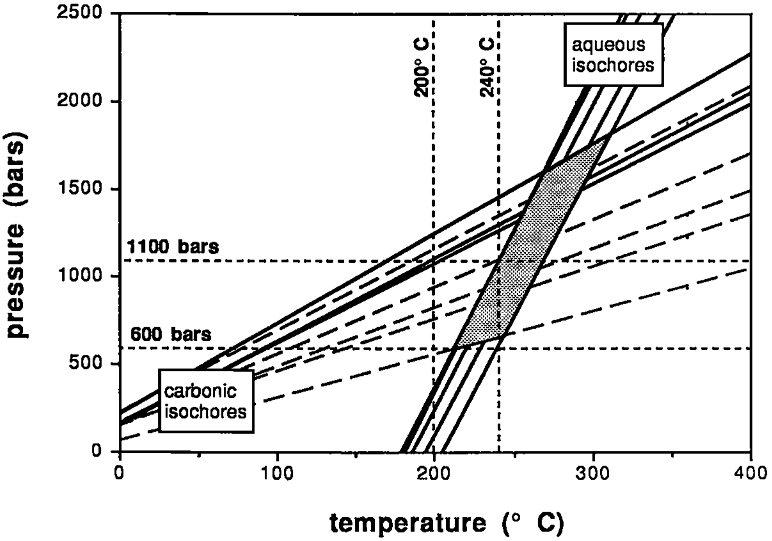

FIG. 14. Isochores for aqueous and carbonic fluid inclusions. Those for inclusions represented by the systems CO_2 and H_2O-NaCl (solid lines) were calculated using the computer program FLINCOR developed by P.H. Brown and distributed by Wiscware. Isochores for CO_2-CH_4 inclusions (long dashes) were calculated using the algorithm of Jacobs & Kerrick (1981) and an unpublished computer program of the second author. The shaded area represents the range of P-T conditions predicted by isochore intersections. The short dashes indicate temperatures estimated from oxygen isotope fractionation between quartz and scheelite and the corresponding pressures predicted by the intersection of these isotherms with isochores for the aqueous and carbonic fluids.

shown in Figure 14. These intersect at temperatures ranging from 210° to 310°C and pressures ranging from approximately 600 to 1800 bars. Assuming, however, that the best estimates of entrapment temperatures are provided by the oxygen isotope data, the corresponding entrapment pressures would be in the range 600 to 1100 bars.

Thus in summary, we estimate the pressure and temperature conditions to have been 600 to 1100 bars and 200° to 240°C, with lower and higher temperatures corresponding to conditions in the subhorizontal and subvertical veins, respectively.

Source of fluid

Although geological evidence presented earlier suggests that the Saint-Robert deposit is genetically related to a granitic pluton, the low temperatures interpreted for vein formation would appear to rule out any significant contribution of orthomagmatic fluids to the ore-forming process. Possible sources for the mineralizing fluids were investigated with the oxygen isotopic data presented above and calculations of the composition of the water that would have been in isotopic equilibrium with the quartz and scheelite samples analyzed. Calculations were performed for temperatures of 240° and 200°C for subvertical and subhorizontal veins, respectively. The resultant $\delta^{18}O_{H_2O}$ values range from -1.4 to +2.9‰ with a mean of +0.4‰ for subvertical veins and from -2.6 to +3.0‰ with a mean of 0‰ for subhorizontal veins (Table 1). These values could represent either seawater or groundwater accumulating in an equatorial environment. The latter interpretation is preferred because of the low salinity of the trapped fluids and is supported by paleomagnetic data, which suggest that this part of the Appalachians was at equatorial latitudes during and shortly following the Acadian orogeny (Briden & Irving 1964, Ma 1958, Opdyke 1962).

Conditions in the source region

As previously discussed, fluids with compositions represented by the aqueous-carbonic inclusions show a wide field of immiscibility at the temperature-pressure conditions estimated for the formation of the deposit. It would, however, be significant in interpreting the controls of mineralization, to know if the ore fluids were initially immiscible, or whether such immiscibility

TABLE 2. REPRESENTATIVE MICROTHERMOMETRIC AND COMPOSITIONAL DATA ON FLUID INCLUSIONS

Aqueous-carbonic inclusions

vein set	origin	Tm CO_2	Th CO_2	Te	Tm ice	Tm C	sal.	Th	Flw	ZCO_2	ZCH_4	ZN_2	dl	dv	XCO_2	XCH_4	XN_2	XH_2O
SZ(sv)	PS	-56.6	9.8	-30	-6.4	6.5	6.6		0.8	1.00			1.01	0.86	0.07			0.93
SZ(sv)	P	-56.7	12.6			6.7	6.3	215	0.8	1.00	0.01		1.01	0.91	0.09	0.00		0.91
CZ(sv)	PS	-57.5	11.2	-19	-6.1	6.7	6.3	234	0.75	0.96	0.04		1.01	0.87	0.10	0.00		0.89
CZ(sv)	PS	-59.2	10.8						0.25	0.22	0.65	0.13		0.24	0.22	0.65	0.13	
CZ(sh)	PS	-64.7	-46.4							0.56	0.36	0.08		0.37	0.56	0.36	0.08	
CZ(sh)	P	-64.6	-51.5							0.45	0.37	0.18		0.33	0.45	0.37	0.18	
NZ(sv)	PS	-56.9	6.8	-31		6	7.5		0.6	0.98	0.02		1.03	0.93	0.20	0.00		0.80
NZ(sv)	P	-59.6	6.5	-27	-5.4	8.5	3.0	227	0.95	0.73	0.27		0.99	0.43	0.01	0.00		0.99
NZ(sh)	PS	-57.3	9.8	-25	-5	8.5	3.0	232	0.8	0.97	0.04		0.99	0.90	0.08	0.00		0.91
NZ(sh)	P	-64.4	-27.5	-27		8.4	3.2		0.85	0.85	0.15		0.99	0.58	0.04	0.01		0.96

Aqueous inclusions

vein set	origin	Te	Tm ice	sal.	Th
SZ(sv)	PS	-27	-2.6	4.3	184.8
SZ(sv)	PS	-28.2	-4	6.4	205.7
SZ(sv)	S	-28	-3.7	6.0	143.4
SZ(sv)	S	-20	-3	4.9	151.3
CZ(sh)	PS	-29.8	-4.3	6.9	
CZ(sv)	S	-30			165

Representative microthermometric and compositional data for aqueous-carbonic, carbonic, and aqueous inclusions. Underlined values represent compositional data derived from Raman spectroscopic analysis. SZ, CZ, NZ refer to South, Centre and North zones; (sv) and (sh) refer to subvertical and subhorizontal veins; P, PS and S correspond to primary, pseudosecondary, and secondary fluid inclusions; sal. refers to salinity, expressed as NaCl wt.% equivalent; Flw is the volumetric fraction of the aqueous liquid in the inclusion at the homogenization temperature of the carbonic phases; dl and dv are the densities of the liquid and vapor. Other terms are defined in the text. A listing of these terms is also given in Ramboz et al. (1985).

was the result of phase separation during vein formation. The data of Takenouchi & Kennedy (1965) and Gehrig (1980) for the system H_2O-CO_2-$NaCl_{6\ \mathrm{wt.\%}}$ (analogous to the one documented at Saint-Robert), show that there is a single fluid phase at temperatures above about 425°C at the pressures estimated for vein formation (600-1100 bars). This temperature decreases slightly with increasing pressure. It is thus quite conceivable that in the source region there was a single homogeneous aqueous-carbonic fluid. This hypothesis can be tested by determining whether or not the aqueous-carbonic fluids represent equilibrium in the system C-O-H. As discussed above, primary and pseudosecondary CO_2-CH_4-bearing inclusions are comparatively common in the Saint-Robert veins. However, according to Holloway (1984), such fluids can only be in equilibrium at geologically unreasonable conditions. Under other conditions, they would coexist with variable proportions of H_2O. Since we have already demonstrated that there was extensive immiscibility at the site of deposition, it might be argued that the disequilibrium represented by these inclusions is simply due to the loss of H_2O during phase separation. If, however, this was the case, then the observed compositions of the carbonic fluid inclusions would be expected to plot in one, or perhaps a limited number of clusters on the CO_2-CH_4 join. The aqueous-carbonic inclusions would be expected to lie along tie-lines joining the H_2O apex to these clusters. An examination of the C-O-H diagrams presented in Figure 15 shows that this is clearly not the case. In all of the sets of veins, the carbonic inclusions are evenly distributed over wide intervals of the CO_2-CH_4 join. In the Centre zone, they extend almost continuously from CO_2 to CH_4. With the exception of the South zone, the compositions of the aqueous-carbonic inclusions, when projected through the H_2O apex to the CO_2-CH_4 join, form a family of tie-lines that covers much of the CO_2-CH_4-H_2O region; in the South zone, most of the aqueous-carbonic inclusions fall along the H_2O-CO_2 join. It therefore follows that the aqueous and carbonic parts of the ore fluid were never in equilibrium. According to experimental studies and studies of geothermal systems, the blocking temperature for equilibrium in the system C-O-H is between 300° and 400°C (*cf.* Giggenbach 1982, Harting & Maass 1980, Ohmoto 1986, Sheppard 1981). It can thus be concluded that temperatures in the source region were probably below 350°C, which in turn indicates that the aqueous-carbonic fluids were also immiscible from the outset.

Significance of the nitrogen

Nitrogen is found only in fluid inclusions in veins (subhorizontal and subvertical) from the Centre zone. These, together with subhorizontal veins from the North zone, also host inclusions with the highest proportions of CH_4 in the carbonic phase(s) (Figs. 10, 11). The proportion of N_2 relative to CO_2

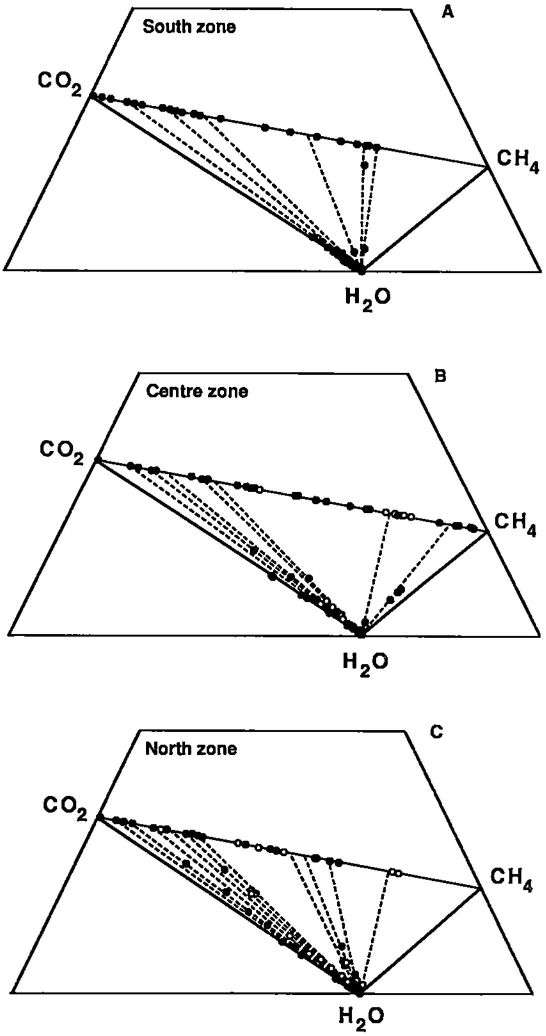

FIG. 15. Compositions of aqueous-carbonic fluid inclusions projected into the system C-O-H. Tie-lines show the compositions of H_2O-CO_2-CH_4 inclusions projected through the H_2O apex to the CO_2-CH_4 join. Closed circles represent subvertical veins, open circles represent subhorizontal veins. See text for further details.

and CH_4 differs markedly between subvertical and subhorizontal veins. In the latter veins, N_2-bearing inclusions have relatively constant proportions of N_2, CO_2 and CH_4 at intermediate values of $X(CH_4)$. In contrast, corresponding inclusions from subvertical veins define a trend from the CH_4 apex, of increasing N_2 with increasing CO_2 in a CO_2:N_2 ratio of approximately 2:1 (Fig. 12). A possible explanation for this trend is that it resulted from the dilution of the N_2-bearing fluid by a separate CH_4-rich fluid.

The most likely origin of the N_2-bearing fluid in the Centre zone veins is the oxidation of NH_4^+ in organic material by circulating, meteoric groundwaters (Bell & Hunt 1963). An alternative source for N_2 is the oxidation of NH_4^+ that may have substituted into the structure of phyllosilicate minerals (Honma & Itihara 1981). The reason why the N_2-bearing fluids were restricted to Centre zone veins is not known. However, the observation that alteration was most pronounced and acidic (argillic alteration) in this zone may indicate that N_2 was released only from rocks that had been strongly altered. Some support for this interpretation is offered by the observation that nitrogen tends to be retained during the degradation of organic matter and is released only at comparatively high metamorphic grades (Kinghorn 1983).

Genetic model

The spatial association of the Saint-Robert deposit with a swarm of felsic dykes and a strong magnetic anomaly, and its location within a large thermal metamorphic aureole, suggest a genetic link with an unexposed granitic stock. The low temperatures, low to moderate pressures and isotopic compositions interpreted for the ore fluids are consistent with a model in which intrusion of a felsic magma initiates a meteoric-water-dominated hydrothermal system and focusses these fluids into suitable higher-level structures, where they deposit their metals.

The high contents of CO_2, CH_4 and N_2 in these fluids are attributed to sedimentary sources. Where the slightly acidic (phyllic alteration) meteoric fluids interacted with calcareous greywacke, they gained CO_2; where they traversed beds rich in organic matter, they gained CO_2 (through oxidation of the organic matter), CH_4, and N_2. The comparatively low initial temperatures of these fluids determined that much of the CO_2, CH_4 and N_2 was released as a separate carbonic fluid, which, although physically entrained in the aqueous phase, was only partially dissolved by it. These low temperatures also ensured that at no stage was equilibrium attained among the various components of the fluids.

The positive correlation between the occurrence of N_2-bearing inclusions and the tungsten content of the veins suggests that the tungsten also may have been derived from source beds rich in organic matter; organic radicals including NH_2 groups are well known for their ability to chelate metals (Manskaya & Drozdova 1968). As suggested earlier for nitrogen, it is possible that tungsten is concentrated in the Centre zone veins because the release of tungsten and nitrogen from the organic matter required particularly acidic fluids. The signature of these fluids, as already noted, could be the argillic alteration, which is restricted to the Centre zone.

The most likely form of dissolved tungsten for the fluid compositions and temperatures interpreted in this study, and at the pH conditions implied by argillic alteration, is the bitungstate ion (HWO_4^-; Wesolowski 1984, Wesolowski *et al.* 1984). According to Wesolowski (1984), increasing pH is the single most important factor leading to the destabilization of this species and hence, scheelite deposition. At the probable ionic strength and pressures of the Saint-Robert fluids, decreasing temperature is not likely to have been a significant cause of scheelite deposition. Indeed, scheelite solubility may actually have increased slightly as temperature decreased (Wesolowski 1984). Whether or not increased calcium activity was a factor in scheelite deposition is difficult to assess. It is probable that there was initially sufficient calcium in solution to account for the tungsten deposited as scheelite, in which case any additional calcium supplied at the site of deposition (*e.g.*, from the wallrocks) would not have increased the amounts of scheelite deposited. On the other hand, most of the calcium in solution would have been in the form of the calcium chloride ion pair, $CaCl_20$, thereby making it unavailable to the tungsten (Williams-Jones & Seward 1989). With decreasing temperature, the ion pair would have destabilized, releasing calcium for deposition as scheelite. Lead, zinc, and silver were almost certainly transported as chloride complexes and could have been deposited in response to either increasing pH or decreasing temperature (Barrett & Anderson 1988, Ruaya & Seward 1986, Seward 1976). No solubility data are available for Bi.

In view of the preceding discussion and the widespread pervasive argillic and phyllic alteration, we propose that mineral deposition was caused by the increase in pH that was associated with neutralization of the fluids as they moved into high-level fractures within calcareous host rocks. It is also possible that additional pH increase was caused by the higher degree of fluid immiscibility, which would have resulted from decreasing pressure and temperature. Some support for increasing pH as a control of deposition is provided by the coexistence of much of the mineralization with calcite, a mineral well known for its tendency to precipitate when pH is increased. In the case of sulfides, decreasing temperature also may have been a factor in mineralization. We propose that the observed distribution of metals was related to stratigraphic control of metal sources and the steeply dipping nature of the strata. These factors served to localize the mineralization in narrow vertical zones at higher elevations but similar stratigraphic levels to the source regions.

Thus, in summary, Saint-Robert is an example of a mesothermal, vein-type polymetallic tungsten deposit, genetically related to an unexposed granitic pluton. Metal leaching and transport are believed to have occurred *via* a meteoric-water-dominated hydrothermal system initiated by the cooling of this pluton. These fluids interacted at depth with organic-matter-rich calcareous sediments, and dissolved metals, sulfur and C–O–H–N volatile species; excess volatiles were transported as a separate phase entrained in the aqueous hydrothermal fluid. The metals were transported to higher structural but similar stratigraphic levels, where scheelite and sulfide deposition occurred in veins, mainly in response to neutralization of the fluids by calcareous host-rocks.

CONCLUSIONS

The principal conclusions of this study are:

1) The ore minerals were deposited by low-salinity aqueous–carbonic fluids; scheelite was deposited by a N_2-bearing aqueous–carbonic fluid.

2) Hydrothermal activity was initiated by the convection of meteoric waters during the cooling of an unexposed felsic stock.

3) The hydrothermal fluids gained variable proportions of CO_2, CH_4, N_2, sulfur and metals (W, Bi, Ag, Pb and Zn) through interaction with organic-matter-rich sediments. This occurred at temperatures $<350°C$, corresponding to conditions for which species in the system C–O–H are in disequilibrium and aqueous and carbonic fluids are immiscible. The excess C–O–H–N volatiles were transported as a separate phase entrained in the aqueous hydrothermal fluid.

4) Ore deposition occurred at temperatures between 200° and 250°C as a result of an increase in pH caused by neutralization of acidic fluids by calcareous wallrocks and possibly limited effervescence of the carbonic phase.

5) The metal zonation was the result of the variable metal contents of the source rocks, and a fluid path that restricted metal transport to the same stratigraphic but higher structural levels.

ACKNOWLEDGEMENTS

Financial support for the research was provided by funds from a federal–provincial mineral development program administered by the Geological Survey of Canada, and NSERC operating and FCAR team grants to AEW-J. Management staff at J.A.G. Mines Ltd. are thanked for their cooperation during the course of this study, and A. Langshur and R. Lemery for their assistance in the field. I. Samson provided invaluable assistance with the operation of the Raman spectrometer. The manuscript benefitted from a critical review by C. Ramboz.

REFERENCES

ARAI, Y., KAMINSHI, G.-I. & SAITO, S. (1971): The experimental determination of the P-V-T-X relations for the carbon dioxide - nitrogen and the carbon dioxide - methane systems. *J. Chem. Eng. Japan* **4**, 113-122.

BARRETT, T.J. & ANDERSON, G.M. (1988): The solubility of sphalerite and galena in 1-5 m NaCl solutions to 300° C. *Geochim. Cosmochim. Acta* **52**, 813-820.

BELL, K.G. & HUNT, J.M. (1963): Native bitumens associated with oil shales. *In* Organic Geochemistry (I.A. Breger, ed.). Pergamon Press, New York (333-366).

BOURNE, J.H. (1989): Pétrographie et géochimie des plutons granitiques d'âges dévonien et crétacé de l'Estrie. *Ministère de l'Énergie et des Ressources du Québec, Rapp.* **ET 88-07**.

BOZZO, A.T., CHEN, J.R. & BORDHUN, A.J. (1973): The properties of the hydrates of chlorine and carbon dioxide. *In* 4th International Symp. on Fresh Water from the Sea (A. Delyannis & E. Delyannis, eds.) **3**, 437-451.

BRIDEN, J.C. & IRVING, E. (1964): Paleolatitude spectra of sedimentary paleoclimatic indicators. *In* Problems in Paleoclimatology (A.E.M. Nairn, ed.). Interscience, New York (199-224).

BURRUSS, R.C. (1981): Analysis of phase equilibria in C-O-H-S fluid inclusions. *In* Fluid Inclusions: Applications to Petrology (L.S. Hollister & M.L. Crawford, eds.). *Mineral. Assoc. Can., Short Course Handbook* **6**, 39-69.

CLAYTON, R.N., O'NEIL, J.R. & MAYEDA, T.K. (1972): Oxygen isotope exchange between quartz and water. *J. Geophys. Res.* **77**, 3057-3067.

CRAIG, H. (1957): Isotopic standards for carbon and oxygen and correction factors for mass-spectrometric analysis of carbon dioxide. *Geochim. Cosmochim. Acta* **12**, 133-149.

______ (1961): Standards for reporting concentrations of deuterium and oxygen-18 in natural waters. *Science* **133**, 1833-1834.

CRAWFORD, M.L. (1981): Phase equilibria in aqueous fluid inclusions. *In* Fluid Inclusions: Applications to Petrology (L.S. Hollister & M.L. Crawford, eds.). *Mineral. Assoc. Can., Short Course Handbook* **6**, 75-100.

GAUTHIER, M. (1985): Synthèse métallogénique de l'Estrie et de la Beauce (secteur sud). *Ministère de l'Énergie et des Ressources du Québec, Rapp.* **MB 85-20.**

GEHRIG, M. (1980): *Phasengleichgewichte und PVT-Daten ternärer Mischungen aus Wasser, Kohlendioxid und Natriumchlorid bis 3 kbar und 550°C.* Doctoral Dissertation, Univ. Karlsruhe; Hochschule Verlag, Freiburg, Germany.

GIGGENBACH, W.F. (1982): Carbon-13 exchange between CO_2 and CH_4 under geothermal conditions. *Geochim. Cosmochim. Acta* **46**, 159-165.

HARRON, G.A. (1976): Métallogénèse des gîtes de sulfures des Cantons de l'Est. *Ministère des Richesses Naturelles, Québec, Rapp.* **ES-27.**

HARTING, P. & MAASS, I. (1980): Neue Ergbnisse zum Kohlenstoff-Isotopenaustausch im System CH_4-CO_2. *In* Mitteilungen Zur z. Arbeitstagung "Isotope in der Natur" (Nov. 1979, Leipzig) **2b**, 13-24.

HIGGINS, N.C. (1985): Wolframite deposition in a hydrothermal vein system: the Grey River tungsten prospect, Newfoundland, Canada. *Econ. Geol.* **80**, 1297-1327.

HOLLISTER, L.S., CRAWFORD, M.L., ROEDDER, E., BURRUSS, R.C., SPOONER, E.T.C. & TOURET, J. (1981): Practical aspects of microthermometry. *In* Fluid Inclusions: Applications to Petrology (L.S. Hollister & M.L. Crawford, eds.). *Mineral. Assoc. Can., Short Course Handbook* **6**, 278-304.

HOLLOWAY, J.R. (1984): Graphite-CH_4-H_2O-CO_2 equilibria at low-grade metamorphic conditions. *Geology* **12**, 455-458.

HONMA, H. & ITIHARA, Y. (1981): Distribution of ammonium in minerals of metamorphic and granitic rocks. *Geochim. Cosmochim. Acta* **45**, 983-988.

JACOBS, G.K. & KERRICK, D.M. (1981): Methane: an equation of state with application to the ternary system H_2O-CO_2-CH_4. *Geochim. Cosmochim. Acta* **45**, 607-614.

KINGHORN, R.R.F. (1983): *An Introduction to the Physics and Chemistry of Petroleum.* John Wiley & Sons, New York.

LITTLE, H.W. (1959): Tungsten deposits of Canada. *Geol. Surv. Can., Econ. Geol. Ser.* **17.**

MA, T.Y.H. (1958): The shiftings in pole-positions with diastrophism since the end of the Cretaceous and the accompanying drift of continents. Research on Past Climate and Continental Drift, Taipei (privately published), 1-176.

MANGAS, J. & ARRIBAS, A. (1988): Hydrothermal fluid evolution of the Sn-W mineralization in the Parilla ore deposit (Caceres, Spain). *Geol. Soc. London* **145**, 147-155.

Manskaya, S.M. & Drozdova, T.V. (1968): *Geochemistry of Organic Substances.* Pergamon Press, Oxford, England.

Ohmoto, H. (1986): Stable isotope geochemistry of ore deposits. *In* Stable Isotopes in High Temperature Geological Processes (J.W. Valley, H.P. Taylor, Jr. & J.R. O'Neil, eds.). *Rev. Mineral.* **16**, 491-559.

Opdyke, N.D. (1962): Paleoclimatology. *In* Continental Drift (S.K. Runcorn, ed.). Academic Press, New York.

Parry, W.T. (1986): Estimation of X_{CO2}, P, and fluid inclusion volume from fluid inclusion temperature measurements in the system $NaCl-CO_2-H_2O$. *Econ. Geol.* **81**, 1009-1013.

Pasteris, J.D., Wopenka, B. & Seitz, J.C. (1988): Practical aspects of quantitative laser Raman microprobe spectroscopy for the study of fluid inclusions. *Geochim. Cosmochim. Acta* **52**, 979-988.

Potter, R.W., II & Brown, D.L. (1977): The volumetric properties of aqueous sodium chloride solutions from 0° to 500°C at pressures up to 2000 bars based on a regression of available data in the literature. *U.S. Geol. Surv., Bull.* **1421-C.**

______, Clynne, M.A. & Brown, D.L. (1978): Freezing point depression of aqueous sodium chloride solutions. *Econ. Geol.* **73**, 284-285.

Ramboz, C., Schnapper, D. & Dubessy, J. (1985): The PV–X–fO_2 evolution of $H_2O-CO_2-CH_4$-bearing fluid in a wolframite vein: reconstruction from fluid inclusion studies. *Geochim. Cosmochim. Acta* **49**, 205-219.

Ruaya, J.R. & Seward, T.M. (1986): The stability of chlorozinc (II) complexes in hydrothermal solutions up to 350°C. *Geochim. Cosmochim. Acta* **50**, 651-661.

Seal, R.R., II, Clark, A.H. & Morrissy, C.J. (1987): Stockwork tungsten (scheelite) - molybdenum mineralization, Lake George, southwestern New Brunswick. *Econ. Geol.* **82**, 1259-1282.

Seward, T.M. (1976): The stability of chloride complexes of silver in hydrothermal solutions up to 350°C. *Geochim. Cosmochim. Acta* **40**, 1329-1341.

Shepherd, T.J. & Waters, P. (1984): Fluid inclusion gas studies, Carrock Fell tungsten deposit, England: implications for regional exploration. *Miner. Deposita* **19**, 304-314.

Sheppard, S.M.F. (1981): Stable isotope geochemistry of fluids. *In* Chemistry and Geochemistry of Solutions at High Temperatures and Pressures (D.T. Rickard & F.E. Wickman, eds.). *Phys. Chem. Earth* **13-14**, 419-445.

So, Chil-Sup,, Rye, D.M. & Shelton, K.L. (1983b): Carbon, hydrogen, oxygen, and sulfur isotope and fluid inclusion study of the Weolag tungsten–molybdenum deposit, Republic of Korea: fluid histories of metamorphic and ore-forming events. *Econ. Geol.* **78**, 1551-1573.

______, Shelton, K.L., Seidemann, D.E. & Skinner, B.J. (1983a): The Dae Hwa tungsten–molybdenum mine, Republic of Korea: a geochemical study. *Econ. Geol.* **78**, 920-930.

Takenouchi, S. & Kennedy, G.C. (1964): The binary stystem H_2O-CO_2 at high temperatures and pressures. *Am. J. Sci.* **262**, 1055-1074.

______& ______ (1965): The solubility of carbon dioxide in NaCl solutions at high temperatures and pressures. *Am. J. Sci.* **263**, 445-454.

Thode, H.G., Monster, J. & Dunford, H.B. (1961): Sulfur isotope geochemistry. *Geochim. Cosmochim. Acta* **25**, 159-174.

Werre, R.W., Jr., Bodnar, R.J., Bethke, P.M. & Barton, P.B. (1979): A novel gas-flow fluid inclusion heating/freezing stage. *Geol. Soc. Am., Abstr. Program* **11**, 539.

Wesolowski, D. (1984): *Geochemistry of Tungsten in Scheelite Deposits: the Skarn Ores at King Island, Tasmania.* Ph.D. thesis, Pennsylvania State Univ., University Park, Pennsylvania.

______, Drummond, S.E., Mesmer, R.E. & Ohmoto, H. (1984): Hydrolysis equilibria of tungsten (VI) in aqueous sodium chloride solutions to 300°C. *Inorg. Chem.* **23**, 1120-1132.

______ & Ohmoto, H. (1986): Calculated oxygen isotope fractionation factors between water and the minerals scheelite and powellite. *Econ. Geol.* **81**, 471-477.

Williams-Jones, A.E. & Seward, T.M. (1989): The stability of calcium chloride ion pairs in aqueous solutions at temperatures between 100° and 360°C. *Geochim. Cosmochim. Acta* **53**, 313-318.

Wopenka, B. & Pasteris, J.D. (1987): Raman intensities and detection limits of geochemically relevant gas mixtures for a laser Raman microprobe. *Anal. Chem.* **59**, 2165-2170.

Received July 14, 1990, revised manuscript accepted January 31, 1991.